

MeV oxygen ion implantation induced compositional intermixing in AlAs/GaAs superlattices

Fulin Xiong^{a)} and T. A. Tombrello

Department of Physics, MS. 200-36, California Institute of Technology, Pasadena, California 91125

C. L. Schwartz and S. A. Schwarz

Bellcore, Red Bank, New Jersey 07701-7040

(Received 20 April 1990; accepted for publication 25 June 1990)

We present in this letter an investigation of compositional intermixing in AlAs/GaAs superlattices induced by 2 MeV oxygen ion implantation. The results are compared with implantation at 500 keV. In addition to Al intermixing in the direct lattice damage region by nuclear collision spikes, as is normally present in low-energy ion implantation, Al interdiffusion has also been found to take place in the subsurface region where MeV ion induced electronic spike damage dominates and a uniform strain field builds up due to defect generation and diffusion. Uniform compositional intermixing of the superlattices results after subsequent thermal annealing when Al interdiffusion is stimulated through recovery of the implantation-induced lattice strain field, the reconstruction and the redistribution of lattice defects, and annealing of lattice damage.

Ion implantation induced compositional disordering or intermixing in III-V compound semiconductor superlattice (SL) structures has attracted increasing interest because of its potential for microfabrication of unique optical and electronic devices.¹⁻⁵ In contrast with dopant diffusion induced SL intermixing,^{6,7} ion implantation offers the versatility to have the disordering at a required depth with the desired electrical activation, spatial selectability, and high reproducibility. In the GaAs/AlAs system, it has been demonstrated that compositional disordering can be realized through ion implantation either with the electrically active implants, such as Zn and Si,^{1,3} with electrically inactive implants, such as Kr, B, and F,^{1,4} or with lattice constituents, like Ga, Al, and As.^{1,4,5} Oxygen is another promising species for the GaAs/AlAs systems; for example, oxygen ion implantation can induce semi-insulating effects in GaAs,^{8,9} and AlGaAs.¹⁰ Recently, Bryan *et al.*¹¹ have reported that, in addition to high-resistivity generation, oxygen ion implantation can simultaneously induce compositional disordering in AlAs/GaAs SLs as well. In fact, oxygen ion implantation has been employed in the fabrication of single quantum well semiconductor laser devices,^{12,13} where high efficiency performance depends on the implantation-induced electrical isolation effect for injection current control, and compositional disordering at the boundaries of the active region (that is, the quantum well) for lateral optical confinement.

Commonly, low-energy ion implantation (LEIM) in the few hundred keV range has been utilized for the disordering process, in which the mechanism is mainly due to implantation-induced lattice damage or inward deep diffusion of impurities introduced in by implantation. High-energy ion implantation (HEIM) in the few MeV range extends the ion-solid interaction into a new regime and provides many additional advantages,^{14,15} such as deep implantation, minimized surface structural damage, and electronic ionization correlated secondary effects. We present in this letter an

investigation of compositional intermixing in AlAs/GaAs superlattices through MeV oxygen ion implantation at low temperature (LT) and subsequently annealing at high temperature (HT). This is compared with LEIM at 500 keV. The results show that, in addition to Al intermixing in the direct ballistic lattice damage region, as is normally present in LEIM, uniform compositional disordering has also taken place in the subsurface region where MeV ion induced electronic damage predominates and a uniform strain field builds up due to defect production, diffusion, and relaxation.

The samples used in this study were 1- μm -thick SLs grown by molecular beam epitaxy (MBE) on a Cr-doped semi-insulating GaAs substrate. The SLs are composed of 25 periods of AlAs (150 Å)/GaAs (250 Å) layers. Implantation was done at the Caltech Tandem Accelerator Laboratory with oxygen ions at energies of 2 MeV or 500 keV for a dose of 1×10^{16} ions/cm². The target holder was maintained at LT with LN₂ cooling (100 K). Subsequent annealing was carried out at 650 °C for 30 min on a graphite hot plate in the proximity-covering format with a GaAs crystal in an ambient Ar gas flow. The oxygen distribution, the degree of Al interdiffusion, and layer intermixing were examined with secondary-ion mass spectrometry (SIMS) at the Bellcore Laboratory. Cesium ions at 8 keV were employed as the primary ions for oxygen profiling, and 15 keV oxygen ions for Al profiling.

The SIMS profiles of ²⁷Al in an unimplanted sample and of ¹⁶O implants in the implanted samples are shown in Fig. 1. The oscillation of the Al signal with a peak-to-valley ratio of about 4.5 in the Al profiles represents a regular AlAs/GaAs superlattice structure. After being annealed at 650 °C for 30 min, the Al profile in an unimplanted sample (its SIMS profile is not plotted here) showed essentially no difference, except for oxidation at the top surface due to uncapped annealing. Oxygen profiles have a distorted Gaussian distribution, indicating a depth range of about 0.65 μm with a full width at half maximum (FWHM) of 0.3 μm for 500 keV ions and 1.85 μm and 0.5 μm for 2 MeV ions. The irregular oscillation of the oxygen depth profiles within the SL region is probably

^{a)} Present address: Gordon McKay Laboratory of Applied Sciences, Harvard University, Cambridge, MA 02138.

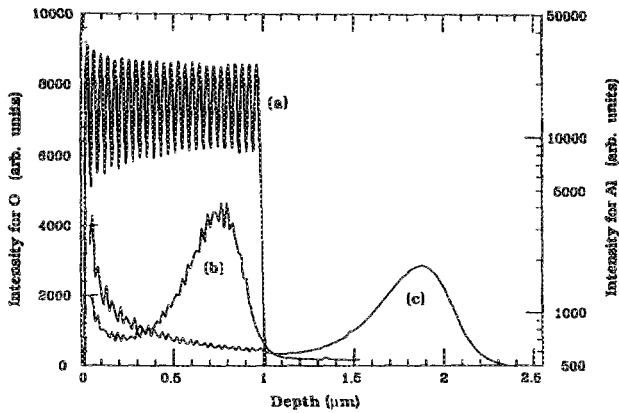


FIG. 1. SIMS profiles of (a) ^{27}Al in the as-grown AlAs/GaAs superlattices, and (b) of ^{16}O in 500 keV and (c) 2 MeV oxygen ion implanted (at doses of 1×10^{16} ion/cm 2) AlAs/GaAs superlattice.

due to the matrix effect in the SIMS measurement.

The Al SIMS profiles of implanted samples are monitored both before and after subsequent HT annealing. In the as-implanted samples, slight Al interdiffusion was observed in both the LEIM and HEIM cases. Presented in Fig. 2 is one profile from a HEIM sample (solid curve), where the Al profile from an unimplanted sample is plotted as a dashed curve for comparison. It is found that the regular Al oscillation remains, but peak-to-valley ratio drops to 4. It behaves very much the same way in the LEIM samples (the profile is not plotted here). The weak change in Al oscillation suggests that Al interdiffusion at this stage is mainly due to nuclear knock-on-induced lattice displacement (or nuclear ballistic damage) during implantation. However, extensive Al interdiffusion has been activated by HT annealing. The corresponding SIMS Al profiles are illustrated in Fig. 3. Significant differences exist between these two samples, although the complete disordering did not take place under the conditions employed. In the LEIM sample [see Fig. 3(a)], the amplitude of Al oscillation has dramatically decreased with the peak-to-valley ratio down to 1.4, which indicates that substantial intermixing has taken place in the AlAs/GaAs SL layers due to implantation and annealing. In most of the surface region, this intermixing is very uniform;

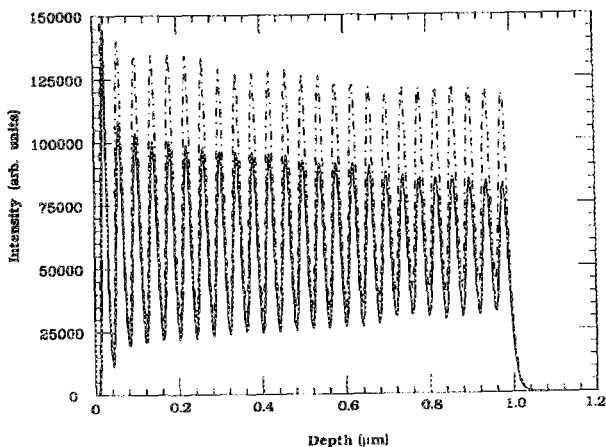


FIG. 2. SIMS depth profile of ^{27}Al in an as-implanted AlAs/GaAs superlattice sample that was implanted with 2 MeV oxygen ions at a dose of 1×10^{16} ions/cm 2 . The Al profile of the unimplanted sample is plotted as a dotted line for comparison.

however, in a few layers near the end of the SLs, the peak value of the Al oscillation has decreased further. This region corresponds to the region where the implanted oxygen ions are deposited (compare to the oxygen depth profile shown in Fig. 1). This decrease implies significant lattice damage- and impurity-related Al inward diffusion due to the existence of implanted oxygen in this region. In the HEIM sample [see Fig. 3(b)], the peak-to-valley ratio of Al oscillation decreases to 1.6, slightly higher than that in the LEIM sample. However, the amplitude remains very uniform over the whole SL region, except for the anomalous distortion of a few layers at the top surface, which is due to the presence of surface oxygen introduced during the uncapped annealing process.

In summary, the results presented above have clearly shown that compositional intermixing in AlAs/GaAs superlattices can be realized by MeV oxygen ion implantation with subsequent HT annealing. This intermixing spreads uniformly throughout the entire subsurface region. Though completed disordering was not observed in either LEIM or HEIM, the results clearly indicate that a dose of 1×10^{16} ions/cm 2 is enough to induce substantial interdiffusion of Al in AlAs/GaAs SLs, which was not realized in the experiments by Bryan *et al.*¹¹ In order to achieve complete disordering, annealing for a longer time or at higher temperature seems to be required, since a processing dependence may

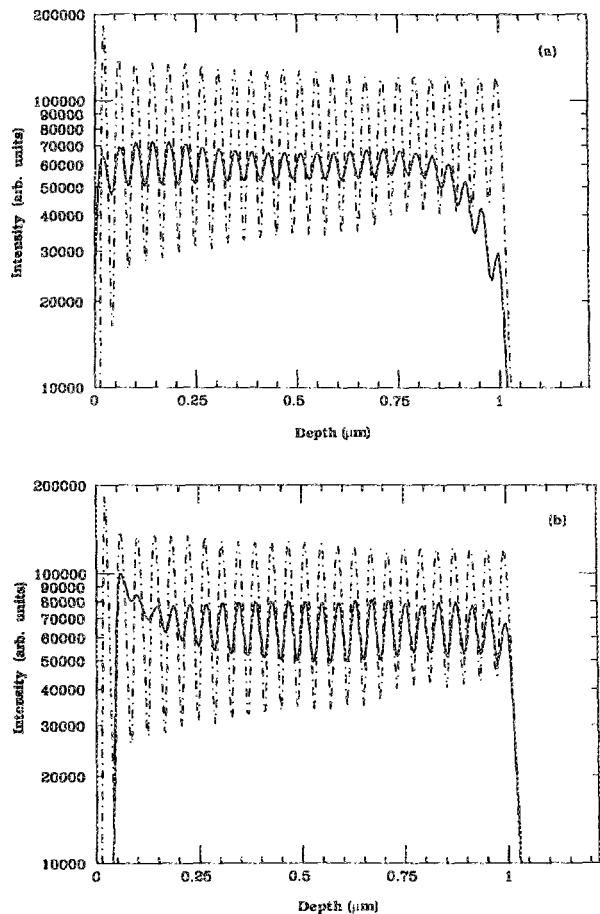


FIG. 3. SIMS depth profile of ^{27}Al in an oxygen ion implanted and subsequently high-temperature-annealed AlAs/GaAs superlattices, (a) 500 keV and (b) 2 MeV. The Al profile of the unimplanted sample is plotted as a dotted line for comparison.

exist, as previously demonstrated by Schwarz *et al.*¹⁶ Our experimental evidence has also convinced us that Al diffusion in the high-energy oxygen ion implanted sample is controlled by a different mechanism than in LEIM. It is suggested that electronic distortion induced by MeV ions in the subsurface region enhances defect diffusion during implantation, which in turn induces a strong uniform lattice strain field in the implanted subsurface region. During the subsequent HT treatment, Al interdiffusion is activated by strain relaxation, defect redistribution, and damage annealing.

It has been shown in our previous work on MeV ion implantation into III-V compound semiconductors¹⁷⁻¹⁹ that lattice damage and disordering in high-energy ion implantation is produced by two distinct processes in different regions: nuclear spike damage around the end of range (EOR) of the ions, and electronic spike damage along most of the ion's path in the surface region. These two processes are closely correlated with the energy loss of an incident ion along its path. The intense energy transfer from ions to lattice atoms due to ion-nucleus collision cascades (nuclear spike) causes substantial lattice atomic displacement and massive production of vacancy-interstitial pairs, resulting in direct structural damage to lattices, as well as the crystalline-to-amorphous structural phase transition. This is the dominant process present in the most cases of LEIM. It appears at the EOR of MeV ions in HEIM, where the incident ions have already lost most of their kinetic energy by interactions with electrons along their paths and slow down into the keV region. But the effect is less pronounced than that by LEIM due to ion energy straggling, which produces a spread in the distribution of implants. A high critical dose for a completed phase transition may be required in this case. The SL compositional disordering taking place under this process is mainly due to ion-induced ballistic intermixing through atomic displacement or due to fast diffusion of active impurities. A strong dependence upon the implantation condition and the geometry is limited to the spatial range around the EOR of the ions or to where diffusing impurities can reach.¹⁶ The electronic spike is produced through ion-electron interactions in the form of electronic ionization and excitation. It spreads along most of the ion's track where electronic energy loss predominates and causes the production of electron-hole pairs, leading to the distortion of the electronic configuration of the lattice. While some electron-hole pairs disappear through quick recombination, an internal electric field may be built up by separation of electrons and holes due to the migration of ionized "free" electrons. For instance, a surface potential may be built up when the ionized electrons accumulate on the surface, leaving the unfilled holes attached to lattice atoms in the subsurface region. This potential, in turn, greatly enhances the migration and diffusion of the lattice defects and the displaced atoms. Finally, this process results in a strong lattice strain field buildup in the subsurface region due to distribution of point defects^{17,19} (about 0.5% to 1.0% in 2 MeV oxygen ion implanted GaAs, which varies with the implantation conditions, such as the ion dose and substrate temperature). During the subsequent HT annealing process, a large amount of energy is released due to the recovery of the implanted-induced lattice strain field

through relaxation or distortion. Implantation-induced defects also redistribute themselves, either by recombination or by developing into extended defects, such as dislocation loops, twins, and stacking faults.¹⁸ All these changes will strongly stimulate diffusion of the residual atoms like Al and Ga under the stoichiometric gradient. The final result of SL compositional disordering is a product of the processes of defect generation and diffusion enhanced by electronic spikes and during implantation and atomic interdiffusion stimulated through strain relaxation and defect reconstruction during annealing. This may explain why the subsequent HT processing is a necessary step to obtain substantial Al interdiffusion. LT implantation can be of help in this process since the "freezing-in" effect induced by LT gives better confinement of lattice damage and defects as well as implants.¹⁶ At LT, there is a tendency to minimize both the possibility of defect recombination and *in situ* dynamic annealing, and thereby, in turn, to preserve lattice damage and buildup of lattice strain in the implanted region, which enhance the diffusion process during annealing.

This work is supported in part by the National Science Foundation grant DMR88-11795. The author (F. X.) is grateful to Dr. H. Wang and Professor Amnon Yariv at Caltech, Professor Hadis Morkoç at University of Illinois, and Dr. T. Venkatesan at Bellcore for their encouragement of this work and their valuable advice.

¹P. Gavrilovic, D. G. Deppe, K. Meehan, N. Holonyak, Jr., J. J. Coleman, and R. D. Burnham, *Appl. Phys. Lett.* **47**, 130 (1985).

²T. Saitoh, T. Yokogawa, and T. Narusawa, *Appl. Phys. Lett.* **55**, 735 (1989).

³T. Venkatesan, S. A. Schwarz, D. M. Hwang, R. Bhat, M. Koza, H. W. Yoon, P. Mei, Y. Arakawa, and A. Yariv, *Appl. Phys. Lett.* **49**, 701 (1986).

⁴Y. Hirayama, Y. Suzuki, and H. Okamoto, *Jpn. J. Appl. Phys.* **11**, 1498 (1985).

⁵Y. Hirayama, Y. Suzuki, S. Tarucha, and H. Okamoto, *Jpn. J. Appl. Phys.* **24**, L516 (1985).

⁶W. D. Laidig, N. Holonyak, Jr., M. D. Camras, K. Hess, J. J. Coleman, P. D. Dapkus, and J. Bardeen, *Appl. Phys. Lett.* **38**, 776 (1981).

⁷N. Holonyak, Jr., W. D. Laidig, M. D. Camras, J. J. Coleman, and P. D. Dapkus, *Appl. Phys. Lett.* **39**, 102 (1981).

⁸P. N. Favennec, G. P. Pelous, M. Bib-net, and P. Baudet, in *Ion Implantation in Semiconductors and Other Materials*, edited by B. L. Crowder (Plenum, New York, 1973), p. 621.

⁹P. N. Favennec, *J. Appl. Phys.* **47**, 2532 (1976).

¹⁰S. J. Pearton, M. P. Iannuzzi, C. L. Reynolds, Jr., and L. Peticolas, *Appl. Phys. Lett.* **52**, 395 (1988).

¹¹R. P. Bryan, M. E. Givens, J. L. Klatt, R. S. Averback, and J. J. Coleman, *J. Electron. Mater.* **18**, 39 (1989).

¹²Fulin Xiong, T. A. Tombrello, H. Wang, T. R. Chen, H. Z. Chen, H. Morkoç, and A. Yariv, *Appl. Phys. Lett.* **54**, 730 (1989).

¹³Fulin Xiong, T. A. Tombrello, H. Wang, T. R. Chen, H. Z. Chen, H. Morkoç, and A. Yariv, *Mater. Res. Soc. Symp. Proc.* **144**, 367 (1989).

¹⁴Fulin Xiong and T. A. Tombrello, *Nucl. Instr. Methods B* **40/41**, 526 (1989).

¹⁵T. A. Tombrello, *J. de Phys. (France)* **C2**, C2-1 (1989).

¹⁶S. A. Schwarz, T. Venkatesan, D. M. Hwang, H. W. Yoon, R. Bhat, and Y. Arakawa, *Appl. Phys. Lett.* **50**, 281 (1987).

¹⁷Fulin Xiong, Ph.D. thesis, Caltech, unpublished (Jan. 1990).

¹⁸Fulin Xiong, S. C. W. Nieh, and T. A. Tombrello, *Ultramicroscopy* **30**, 242 (1989).

¹⁹Fulin Xiong, C. J. Tsai, T. Vreeland, and T. A. Tombrello (unpublished).